Available online at www.sciencedirect.com
ScienceDirect
Polymer 47 (2006) 6560–6566
polymer
www.elsevier.com/locate/polymer

Decreased oxygen inhibition in photopolymerized acrylate/epoxide hybrid polymer coatings as demonstrated by Raman spectroscopy

Ying Cai, Julie L.P. Jessop*

Department of Chemical and Biochemical Engineering, University of Iowa, 4133 Seamans Center, Iowa City, IA 52242, United States

Received 5 June 2006; received in revised form 7 July 2006; accepted 17 July 2006

Abstract

Photopolymerization systems based on hybrid monomer 3,4-epoxy-cyclohexylmethyl methacrylate (METHB) were studied to investigate the oxygen inhibition effects on the conversion and polymer properties in films and coatings. METHB contains epoxide and methacrylate functional groups, which undergo cationic and free-radical photopolymerization, respectively. The conversion of both groups was obtained by Raman confocal microscopy as a function of depth. Initiator system compositions were varied and shown to affect the depth profile. The methacrylate group conversion was low at the surface due to oxygen inhibition. When both reactions were present, a cross-linked network formed and reduced oxygen sensitivity. At depths greater than the oxygen-diffusion-affected region, both functional groups' conversions did not show depth dependence. In addition, epoxide groups continued reacting after light was shuttered and reached a higher and more homogeneous conversion. These systems exhibit lower sensitivity to oxygen and offer advantages such as increased cure speed and improved film-forming properties compared to free-radical systems.

Keywords: Photopolymerized epoxide/acrylate hybrid coatings; Raman confocal microscopy; Depth-profiling

1. Introduction

Photopolymerization has drawn great attention due to its advantages of fast curing speeds at room temperature, energy efficiency, and low concentration of volatile organic compounds. Applications of photopolymerization include films and coatings, inks, adhesives, fiber optics, and dental composites [1,2]. Free-radical and cationic photoinitiation are the two main types of mechanisms used in the industry. Acrylates, which undergo free-radical polymerization, exhibit high reaction rates and offer a large selection of monomers and initiators; while epoxides, which undergo cationic ring-opening photopolymerization, do not suffer from oxygen inhibition and exhibit low toxicity and shrinkage. Hybrid photopolymerization systems, which contain two types of functional groups, have arisen in recent years. For example, free-radical and cationic hybrid photopolymerization systems have been reported by mixing acrylate with epoxide [3–6] or vinyl ether [5,7,8] monomers and by synthesizing monomers with both epoxide and vinyl ether moieties [9]. This study focuses on hybrid monomers bearing both acrylate and epoxide functionalities, which have tremendous promise for solving the oxygen inhibition and moisture problems that plague free-radical and cationic polymerizations, respectively; however, there is an important need for fundamental knowledge about the reactions in these systems. These so-called hybrid photopolymerizations combine the advantages of these two reaction pathways and offer better processing properties, less shrinkage, lower sensitivity to both oxygen and moisture, and improved adhesion and flexibility.

1.1. Oxygen inhibition effect upon free-radical photopolymerization

Free-radical photopolymerization is known to be inhibited by molecular oxygen, which can quench the excited triplet state photoinitiator molecules and scavenge the initiator and

* Corresponding author. Tel.: +1 319 335 0681; fax: +1 319 335 1415.
E-mail address: julie-jessop@uiowa.edu (J.L.P. Jessop).

0032-3861/$ - see front matter © 2006 Elsevier Ltd. All rights reserved.
doi:10.1016/j.polymer.2006.07.031

polymer radicals [1,2,10]. This problem has limited the application of free-radical photopolymerization in thin films and coatings. Thus, efforts have been focused on understanding the mechanism of oxygen inhibition towards free-radical polymerization, addressing this issue, enabling the application, and improving the product quality. Different approaches have been used to solve the free-radical sensitivity to oxygen: expensive inerting equipment, waxes, or shielding films can be used to prevent oxygen from entering the system; higher concentration of free-radical initiator or high intensity irradiation sources to produce a larger number of radicals to consume the oxygen faster and allow the polymer chains grow [11,12]; and the addition of other chemical additives, such as amines, to capture the oxygen [11–14]. However, the above methods increase the manufacturing cost or even result in further problems in the products. For example, high concentrations of photoinitiator will decrease the light penetration to the bottom of the coating and result in low and non-homogeneous conversion, which may lead to inferior adhesion properties. Hybrid photopolymerization systems attempt to decrease the oxygen sensitivity of the formulation by introducing oxygen-insensitive epoxide functional groups. Although the epoxide ring reacts more slowly than acrylates, the cationic active centers exhibit ''living'' characteristics [10]. Thus, the conversion of the epoxides increases even after turning off the illumination source. The increased conversion will contribute to better physical properties like surface hardness, adhesion and modulus.

1.2. Real-time Raman spectroscopy and Raman confocal microscopy

To obtain good surface and physical properties for coatings and films, a high degree of conversion is needed. For a free-radical photopolymerization system reacting in air, the reaction is inhibited until the dissolved oxygen has been consumed as low as 10^{-5} M [11]; thus, an induction period will be present. Once the polymerization begins, additional radicals are prevented from contributing to polymer chain propagation as oxygen continues to diffuse into the system. Under these conditions, thin films are not able to cure, and thicker films exhibit tacky surfaces with higher conversion beyond the oxygen-diffusion-affected region.

In-situ investigations of photopolymerizations have been carried out using photo-differential scanning calorimetry (PDSC) [4,6] and real-time infrared (RTIR) [3,6], real-time near infrared (NIR) [7], and Raman [15] spectroscopies. PDSC only measures the bulk conversion of the entire sample and cannot differentiate the conversion of different functional groups; thus, it is not suitable for hybrid systems in which two simultaneous reactions occur. RTIR spectroscopy requires special thin film sample preparation; while NIR requires a thick film and provides bulk or macroscopic conversions. Since initiation light absorption and atmospheric effects are a function of depth and can result in a heterogeneous conversion distribution, these methods cannot provide highly resolved microscopic conversion and chemical composition information. In this study, real-time Raman spectroscopy was used to monitor the overall reaction, and then the resulting cured coating samples were investigated by Raman confocal microscopy, a non-destructive method, to obtain profiles of functional group conversions at various sample depths. The Raman scattering technique is based upon changes in the wavelength of the incident light after interaction with the rotational and vibrational energy levels in molecules and is particularly well suited for the detection of chemical bonds and their changes during reaction. The combination of microscopy and Raman spectroscopy greatly improves the spatial resolution, and the depth resolution can be further improved by introducing a confocal arrangement. In this arrangement, the chemical composition at a given depth can be obtained using a pinhole in the back image plane of the microscope objective to filter out Raman effects above and below the sampling plane. Thus, an optical slice of the sample can be obtained without physically touching the sample. This technique has been used for depth-profiling different multilayer and photo-curing polymer coatings and films [16]. Raman microscopy can identify areas 10 times smaller than can be determined by FTIR microscopy, providing better resolution for surface and depth investigations. It is also able to investigate depths up to several tens of microns, which is much greater than with attenuated total reflectance (ATR) FTIR spectroscopy (couple microns) [17]. Mathematical models have been developed to relate the experimental depth with the true focusing point to improve depth resolution and spatial accuracy, which worsens with increasing depth [18–20]. In this study, quantitative assessment is most crucial at the near surface (0–15 μm); however, since the spatial accuracy is still relatively reliable in this region, these models were not used to obtain further depth determination.

In this study, the conversion depth profiles of hybrid systems and traditional free-radically cured systems demonstrate the effect of oxygen upon the microscopic chemical composition of the coatings and films. By combining this information with real-time reaction, kinetic information and the macroscopic physical properties, a better understanding of how the reactions of the epoxide functionality in these hybrid systems reduces the oxygen sensitivity and improves the physical properties of the resulting photopolymer is achieved. This will ultimately facilitate optimization of formulations and reaction conditions for thin film and coating applications.

2. Experimental

2.1. Materials

The hybrid monomer 3,4-epoxy-cyclohexyl-methyl methacrylate (METHB, Daicel) (Fig. 1), which contains a methacrylate double bond and a cycloaliphatic epoxide ring, was used

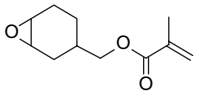

Fig. 1. Molecular structure of hybrid monomer METHB.

in this study. The α-cleavable free-radical photoinitiator 2,2-dimethoxy-2-phenyl-acetophenone (DMPA, Aldrich) and the cationic photoinitiator diaryliodonium hexafluoroantimonate (DAI, Sartomer) were used to initiate the reactions of C═C double bonds and epoxide rings, respectively. All materials were used as received.

2.2. Methods

2.2.1. Raman spectroscopy

Real-time Raman spectra were collected using the Mark II holographic fiber-coupled stretch probehead (Kaiser Optical Systems, Inc.) attached to the HoloLab 5000R modular research Raman spectrograph. A 10× non-contact sampling objective with a 0.8-cm working distance was used to deliver ~200-mW 785-nm near-infrared laser intensity to the sample, thereby inducing the Raman scattering effect. The exposure time for each spectrum was 500 ms, and the time interval between data points was ~700 ms. Samples were cured at room temperature in sealed 1-mm ID quartz capillary tubes using the Acticure® Ultraviolet/Visible Spot Cure system (EXFO Photonic Solutions, Inc.). This system is equipped with a high pressure 100-W mercury vapor short arc lamp; the light intensity was set to 100 mW/cm^2.

A Leica DMLP optical microscope with confocal optics attached to the HoloLab 5000R modular research Raman spectrograph (Kaiser Optical Systems, Inc.) was used to obtain spectra of monomer and depth profiles of photopolymer coatings. A combination of 785-nm single-mode excitation fiber and 15-μm collection fiber was used for all microscopic studies. A 10× objective with numerical aperture equal to 0.25 and with 5.8-mm working distance was used to study the monomer. The laser beam delivered from the 10× objective to the sample was ~9 mW in intensity for microscopic studies. The exposure time for monomer spectra was 5 s. For depth-profiling studies, the monomer mixture was spread on a quartz slide using a razor blade and photopolymerized for 45 min to reach the highest conversion with the Acticure® system at a light intensity of 100 mW/cm^2 under ambient conditions. The thickness of the finished coatings was about 100 μm. A 100× objective with numerical aperture equal to 0.9 and with 0.27-mm working distance was used. This confocal setup provides a spot size of 1.5 μm and depth resolution of 3 μm. The exposure time for depth-profiling studies was set to 120 s to optimize the signal-to-noise ratio (*S/N*). Raman spectra of the coatings were taken starting from the sample surface to ~60 μm within the sample using 4- or 5-μm step sizes to ensure isolated sampling volumes.

The Raman spectrum of METHB was acquired first to identify bands in the fingerprint region that could be used to calculate conversion (see Fig. 2). The reactive band representing the methacrylate C═C double bond is located at 1640 cm^{-1} and is associated with the C═C stretching vibrations [21,22]; the reactive band representing the epoxide ring is located at 790 cm^{-1} and is associated with the symmetric epoxide ring deformation [21,23]. An internal reference band was selected at 605 cm^{-1}, which represents the skeletal bending of the non-reactive methacrylate CC═O group [22]. The peak areas under each band were integrated and used to calculate the concentration of related functional groups. Since the spectral baselines and the reference band intensity remained constant in the real-time studies, the conversion of each functional group was calculated by ratioing the concentration of the functional group at any given time [$A_{rxn}(t)$] to the initial concentration [$A_{rxn}(0)$]:

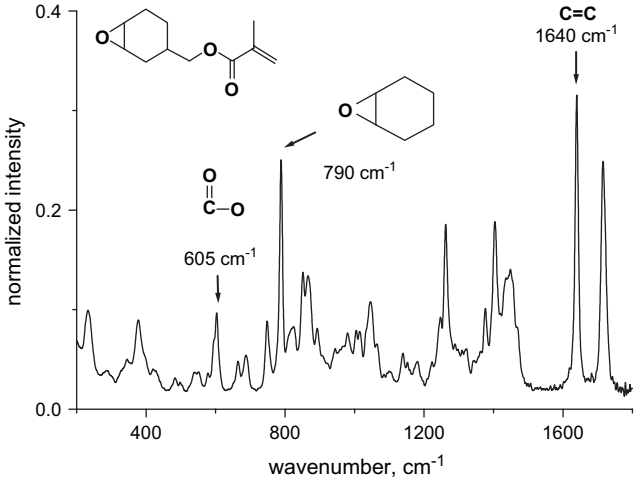

Fig. 2. Characteristic peaks in Raman spectrum of hybrid monomer METHB: internal reference band at 605 cm^{-1}, epoxide ring reactive band at 790 cm^{-1}, and C═C double bond reactive band at 1640 cm^{-1}.

$$\text{conversion, } \alpha = 1 - A_{rxn}(t)/A_{rxn}(0) \quad (1)$$

These results were compared with the conversions calculated using peak areas resolved after taking the second derivative of each spectra using first the chosen characteristic peaks (i.e., 1640 and 790 cm^{-1}) and then the other peaks associated with the same functional groups (e.g., 1410 cm^{-1} for the C═C). The differences between these methods were within the experimental error for this specific monomer, so the results are all reported using Eq. (1). In the depth-profiling studies, the internal reference band was used to eliminate the effect of the decreasing *S/N* as the sampling depth increased and to enable comparison of measurements at different times:

$$\text{conversion, } \alpha = 1 - \frac{A_{rxn}(t)/A_{ref}(t)}{A_{rxn}(0)/A_{ref}(0)} \quad (2)$$

2.2.2. Physical property testing

Coatings prepared in the same way as for the depth-profiling studies were tested to obtain surface hardness, glass transition temperature (T_g) and storage modulus. The surface quality was determined by the film hardness by pencil test based on ASTM D3363-00. The coatings were removed by razor blade from the substrate to obtain free films, which were tested by a Q800 Dynamic Mechanical Analysis (TA Instruments) using the film tension clamp. A temperature ramp from −80 °C to 250 °C at a frequency of 1 Hz and 3 °C/min ramping rate was performed on the film. The T_g of the films

was determined by the tan δ peak. Following this, the storage modulus of each film was obtained from the linear portion of the stress–strain curve in a stress–strain test at 120 °C.

3. Results and discussion

This study investigated the real-time reaction kinetics of METHB, conversion of the methacrylate C=C double bond and epoxide ring as a function of depth in the cured METHB coating, and the physical properties of the resulting coatings and films. Free-radical initiator only and dual-initiator systems were studied, and the response of these two formulations to oxygen was compared.

3.1. Free-radical initiator only system

First, METHB with only the free-radical photoinitiator present was studied using Raman spectroscopy to show the oxygen sensitivity of traditional acrylate systems. Since only DMPA was used to initiate the methacrylate C=C reaction, the resulting polymers are linear chains. Three different initiator concentrations were used to compare the oxygen sensitivity of formulations (see Fig. 3). The 0.25 wt%-DMPA formulation was photopolymerized in a nitrogen-purged chamber and served as the control experiment to compare the oxygen-diffusion effects at the coating surface. As shown in Fig. 3 (left), a higher concentration of DMPA resulted in higher reaction rate, higher conversion of C=C double bond, and shorter induction period. The resulting photopolymer coatings were then studied by Raman confocal microscopy (Fig. 3, right). The control experiment had a homogeneous, high conversion and did not show any dependence upon depth even with a lower initiator concentration. However, both coatings photopolymerized at ambient conditions showed low conversion (only 40–50%) at the surface ($z < 15$ μm), which matched the physical condition of the coatings (i.e., tacky surfaces), because oxygen continues to diffuse into the coating during cure and consumes the free-radical active centers. Thus, this surface layer was designated as the oxygen-diffusion-affected region. As viscosity increases during polymerization, it becomes more difficult for oxygen to penetrate throughout the coating, facilitating higher final conversion values at deeper levels. Thus, the conversion in free-radical initiator only systems increases as the depth increases. In the 0.5 wt%-DMPA formulation, the conversion gradually increased with depth until it reached a plateau value around $z = 15$ μm; however, the 1 wt%-DMPA formulation exhibited a sudden increase of conversion from 50% at $z = 10$ μm to ~85% at $z = 15$ μm. This behavior is due to the higher concentration of initiator, which produces a greater number of active centers and retards the diffusion of oxygen. The conversion did not show a dependence on the depth beyond the oxygen-diffusion-affected region, at which point it agreed well with the ultimate conversion measured in the real-time Raman studies. Thus, the difference in conversion between the surface and the bulk is caused by atmospheric oxygen and not by a lack of initiation light penetrating into the sample. Although the initiator concentration can improve the surface methacrylate C=C bond conversion, the low C=C conversion and tacky surface in thin films and coatings will be difficult to overcome as long as oxygen is present.

3.2. Dual-initiator system

Coatings with METHB and four different combinations of the free-radical initiator DMPA and the cationic initiator DAI were then studied to prove that the hybrid system may address the oxygen inhibition problem. This system exhibits cross-linking since the polymer chains can be connected via the epoxide or methacrylate reactive bonds. Thus, the ultimate conversions of the methacrylate C=C double bond and epoxide ring measured by real-time Raman monitoring are about 70% and 10%, respectively (see Fig. 4). The formulations with the higher concentration of DMPA resulted in faster

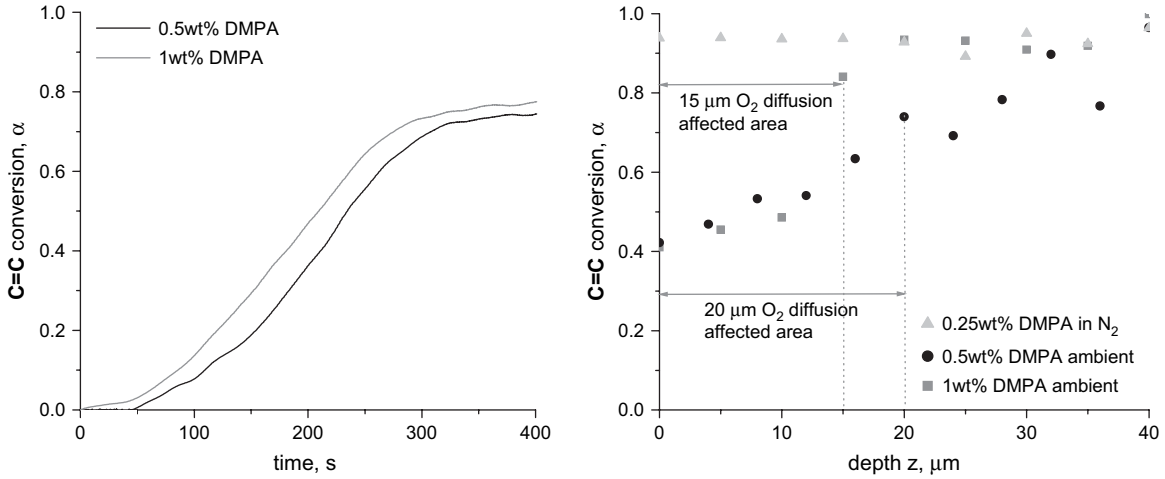

Fig. 3. Conversion profile (left; by real-time Raman spectroscopy) and depth profile (right; by Raman confocal microscopy) of METHB photopolymerized to ultimate conversion with free-radical initiator only. Samples were cured with 100 mW/cm^2 initiation light intensity either at room temperature in a N_2-purged chamber or at ambient conditions.

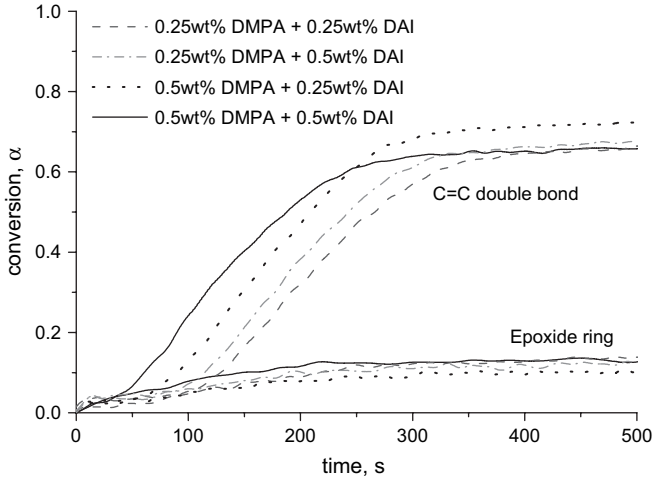

Fig. 4. Conversion profiles of METHB (by real-time Raman spectroscopy) photopolymerized with dual-initiation system at ambient conditions and 100 mW/cm^2.

reaction rate and shorter induction period of C═C double bond compared with the DMPA-only systems. With the same amount of DMPA, the systems with higher concentration of DAI had shorter induction period, but similar reaction rate after the polymerization started. This is because radicals generated during the production of the cationic active center (Eq. 3) can consume some oxygen, although they are not able to initiate the free-radical polymerization of the methacrylate at low temperatures. This behavior of the free radicals was reported by Lin and Stansbury [7] and was confirmed in formulations using only DAI, which were performed as part of this study.

$$\mathrm{Ar_2I^+X^-} \xrightarrow{h\nu} [\mathrm{Ar_2I^+X^-}]^* \rightarrow \mathrm{Ar^\bullet} + \mathrm{ArI^{\bullet+}X^-} \xrightarrow{\mathrm{RH}} \mathrm{ArI} + \mathrm{R^\bullet} + \mathrm{H^+X^-} + \mathrm{Ar^\bullet} \quad (3)$$

However, no significant difference was seen for the epoxide ring reactions among these four formulations since epoxide ring groups react more slowly than the double bonds. In formulations with only 0.5 wt% DAI photopolymerized under the same reaction conditions, the conversion of the epoxide ring reached 20% after 600 s of illumination. Thus, the mobility of the cationic reactive centers was restricted due to vitrification resulting from the high conversion of the C═C double bonds and cross-linking.

In the depth profiles of these samples, the methacrylate bond conversion at the surface increases 15–30% (see Fig. 5, left) from 0 to 12 μm, while the conversion of the epoxide rings drops 25–35% over the same length scale (see Fig. 5, right). In addition, the cross-linked hybrid polymers had non-tacky and smooth surfaces, even though the conversion of the methacrylate bonds was not high. This surface hardness is attributable to the presence of the reacted epoxide rings. The coatings with higher concentration of DMPA showed a higher conversion of C═C double bond and a lower conversion of epoxide ring at the near surface. Compared with the conversion of C═C double bond for the system containing 0.5 wt% DMPA, the conversion of the methacrylate bonds in the dual-initiator system was ~20% higher at a 12-μm depth. The reaction of epoxide rings effectively decreases oxygen diffusion from the air interface to the coating interior, facilitating increased conversion. At depths greater than 12 μm, the methacrylate bond conversion of the dual-initiator system is about 70% and is again comparable with real-time results. As in the free-radical initiator only system, the depth-profile patterns of dual-initiator systems are similar: a gradual increase in the conversion for lower concentrations of DMPA and a sudden increase for higher concentrations.

The cationic active center is known to be long lived after the initiation light is shuttered [24]. Thus, only the photodecomposition of the initiator requires initiation light, and the propagation or chain-growth steps are independent of the light. Ideally, polymerization will continue until no monomer or counterion can access the active center. The extent of the dark polymerization of the epoxide ring is highly dependent on the free volume and the activity of the active center. To investigate the dark-curing characteristic of the epoxide ring, the coating samples were left on the Raman confocal

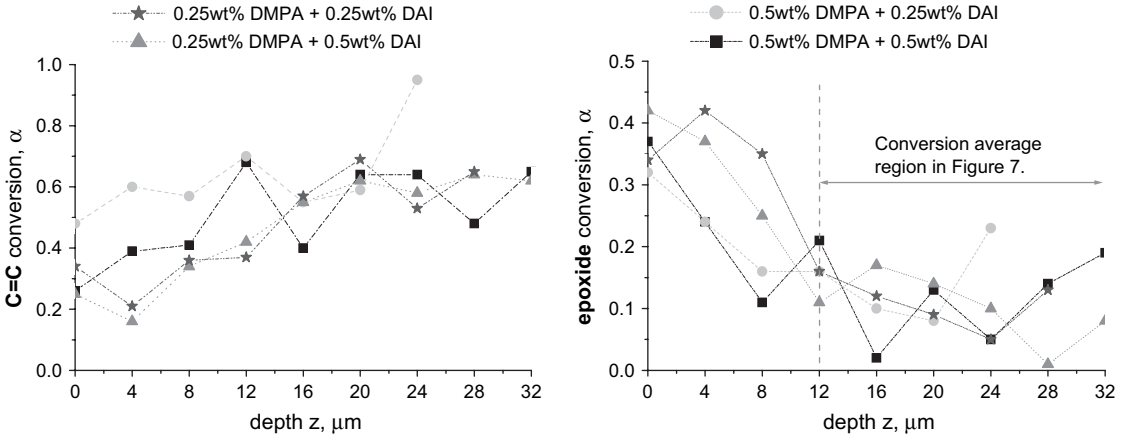

Fig. 5. Depth profiles of C═C double bond (left) and epoxide ring (right) obtained by Raman confocal microscopy for METHB coatings photopolymerized with dual-initiator systems at ambient conditions and 100 mW/cm^2.

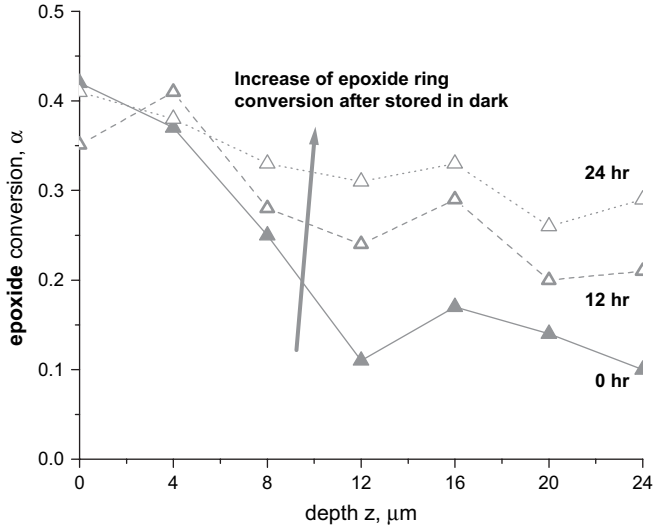

Fig. 6. Depth profiles (at 0, 12 and 24 h after initiation light shuttered) of epoxide ring obtained by Raman confocal microscopy for METHB coating photopolymerized by 0.25 wt% DMPA and 0.5 wt% DAI dual-initiator system at ambient conditions and 100 mW/cm^2.

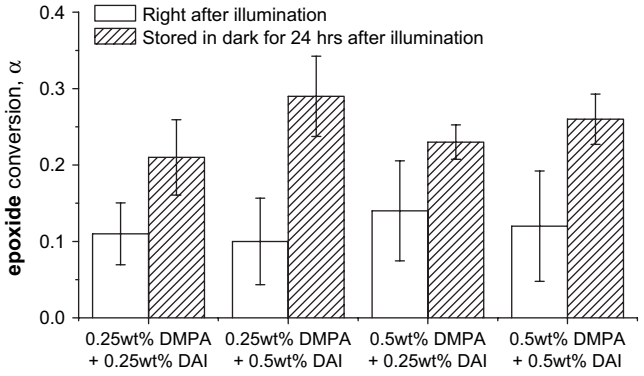

Fig. 7. The average conversion of epoxide ring at depths >12 μm in METHB coatings photopolymerized with dual-initiator systems at ambient conditions. Conversions were obtained after illumination and after 24-h dark storage.

microscope stage for 48 h after illumination ceased. The depth profiles were obtained after dark storage at 12, 24, and 48 h (an example of these results is shown in Fig. 6). In the first 24 h of storage, all samples showed a dramatic increase in epoxide ring conversion (5–15% after 12 h and 5–8% more after another 12 h) at depths greater than 4 μm. The conversions increased until they were slightly lower than the conversion at the surface. Since the mobility of active center is restricted by the polymer network when the cross-linking density increased, no significant change in conversion appeared after the second 24 h of storage. In Fig. 7, the average conversions of epoxide rings at the depths greater than 12 μm (highlighted in Fig. 5, right) were compared among the four formulations. The systems with the higher concentration of DAI (0.5 wt%) showed more conversion than the lower concentration systems since more active centers were generated. In addition, the standard deviations of the conversion after storage are smaller than those calculated at 0 h, indicating a more homogeneous conversion at later times. Thus, the conversions reached final values that are determined by the active center concentration and network restrictions. The dark-curing behavior can increase the cross-linking density and impact the physical properties of the coatings.

3.3. Physical property tests

In industry, the physical properties of films and coatings must be tailored to the ultimate application. Hence, physical property tests were carried out to determine the impact of formulation and its response to oxygen. All coatings were stored in the dark for 48 h to ensure that no substantial reaction of the epoxide rings occurred while samples were tested under elevated temperatures.

All four dual-initiator formulations were tested by pencil hardness and DMA tests (see Table 1). As observed in the depth-profile studies, the formulations containing only free-radical initiator had low conversion on the surface. The surfaces of these formulations were tacky due to oxygen inhibition and could not be tested by DMA. However, the reaction of epoxide rings compensate for the low surface conversion of methacrylate C=C bonds and increase the surface hardness. Although all formulations containing both free-radical and cationic initiators showed 6H gouge hardness, the four formulations displayed different depth profiles, which in turn impacted other physical properties of the coatings. In general, higher concentrations of one or both initiators provided better surface quality. There was little difference in the T_g of the four formulations due to similar polymer structure and conversion in the bulk coating. However, differentiation among the four formulations was made at the extremes. For example, the T_g of the 0.5 wt% DMPA and 0.5 wt% DAI formulation is 8 °C higher than the T_g of the formulation with only 0.25 wt% DMPA and 0.25 wt% DAI. In addition, the cross-linking

Table 1
Comparison of physical properties of the resulting coatings from free-radical only initiator and dual-initiator systems

Initiator system		Pencil hardness		Glass transition temperature (°C)	Storage modulus at 120 °C (MPa)
		Gouge	Scratch		
Free-radical initiator only	0.5 wt% DMPA	Tacky surface		N/A	N/A
	1 wt% DMPA			N/A	N/A
Dual-initiator system	0.25 wt% DMPA + 0.25 wt% DAI	6H	3H	96	434
	0.25 wt% DMPA + 0.5 wt% DAI	6H	4H	103	775
	0.5 wt% DMPA + 0.25 wt% DAI	6H	4H	101	595
	0.5 wt% DMPA + 0.5 wt% DAI	6H	5H	104	770

density of each formulation is different and, as shown in Eq. (4), is directly proportional to the measured storage modulus [25]:

$$\nu_e = \frac{E'}{3RT} \tag{4}$$

where ν_e is the cross-link density, E' is the storage modulus, R is the ideal gas constant, and T is the temperature (K) at which E' is obtained. The kinetic studies and depth profiles show non-homogeneous conversions and low epoxide ring conversion, suggesting a low cross-linking density in the resulting photopolymers. By comparing the storage moduli in the rubbery plateau region of these four coatings, the relative changes in cross-linking density can be determined [26]. Because of the heterogeneous conversions and cross-linking densities within each sample, 120 °C was chosen for the storage modulus tests to facilitate comparison of the cross-linking densities among samples. This choice accommodated the 0.25 wt% DMPA and 0.25 wt% DAI formulation, which had a short rubbery plateau that spanned ~40 °C. In the DMA temperature-ramping studies, T_g, modulus and the length of the rubbery plateau increased with increasing DAI concentration, indicating a greater average extent of cross-linking. This physical picture coincides with the results shown in Fig. 7, which shows higher final conversions of the epoxide ring for formulations with 0.5 wt% DAI. Thus, the surface qualities of the polymer coatings can be significantly improved by the initiation of both functional groups, and the thermal and mechanical properties can be influenced by the relative ratio of the two photoinitiators.

4. Conclusion

Real-time Raman spectroscopy was able to monitor simultaneously the reaction of C=C double bonds and epoxide rings in hybrid systems. The conversion (and ultimately the reaction rate) was influenced by the initiation system. By choosing single- or dual-initiator systems, a homopolymer or cross-linking polymer can be produced. The conversion differences of C=C double bond and epoxide ring at the surface and in the bulk of coatings cured in ambient conditions were quantitatively determined by Raman confocal microscope without destroying the sample. The conversion depth profile showed a strong dependence upon the initiation system. The oxygen-diffusion-affected region in the dual-initiator system is narrower than in the free-radical initiator only system. The dark polymerization behavior of epoxide ring has also been demonstrated. The conversion of epoxide ring can double after 24-h dark storage and reach a more homogeneous final value throughout the sample. The physical properties of the resulting coatings also depended on the initiation system. The cross-linking network developed by inducing the cationic photopolymerization reduced the oxygen inhibition problem and offered better surface properties. A higher concentration of initiators, especially the cationic initiator, improved the coating surface hardness and film modulus.

Acknowledgements

This material is based upon the work supported by the National Science Foundation under Grant No. 0133133 and the University of Iowa. We would like to acknowledge Daicel and Sartomer for providing the materials used in this study.

References

[1] Fouassier JP. Photoinitiation, photopolymerization, and photocuring: fundamentals and applications. New York: Hanser Publishers; 1995.
[2] Koleske JV. Radiation curing of coatings. West Conshohocken: ASTM International; 2002.
[3] Decker C, Nguyen Thi Viet T, Decker D, Weber-Koehl E. Polymer 2001; 42:5531.
[4] Oxman JD, Jacobs DW, Trom MC, Sipani V, Ficek B, Scranton AB. Journal of Polymer Science Part A Polymer Chemistry 2005;43:1747.
[5] Cho JD, Hong JW. Journal of Applied Polymer Science 2004;93:1473.
[6] Dean KM, Cook WD. Polymer International 2004;53:1305.
[7] Lin Y, Stansbury JW. Polymer 2003;44:4781.
[8] Dean KM, Cook WD, Zipper MD, Burchill P. Polymer 2001;42:1345.
[9] Rajaraman SK, Mowers WA, Crivello JV. Novel hybrid monomers bearing cycloaliphatic epoxy and 1-propenyl ether groups. Macromolecules 1999;32:36.
[10] Odian G. Principles of polymerization. 3rd ed. New York: John Wiley & Sons, Inc.; 1991.
[11] Decker C, Jenkins AD. Macromolecules 1985;18:1241.
[12] Fouassier JP, Rabek JF, editors. Radiation curing in polymer science and technology—volume III: polymerisation mechanisms. New York: Elsevier Applied Science; 1993.
[13] Miller CW, Hoyle CE, Jonsson S, Nason C, Lee TY, Kuang WF, et al. Photoinitiated polymerization. ACS Symposium 2003;847:2.
[14] Gou LJ, Coretsopoulos CN, Scranton AB. Journal of Polymer Science Part A Polymer Chemistry 2004;42:1285.
[15] Nelson EW, Scranton AB. Journal of Polymer Science Part A Polymer Chemistry 1996;34:403.
[16] Schrof W, Beck E, Etzrodt G, Hintze-Brüning H, Meisenburg U, Schwalm R, et al. Progress in Organic Coatings 2001;43:1.
[17] Scherzer T. Vibrational Spectroscopy 2002;29:139.
[18] Everall NJ. Applied Spectroscopy 2000;54:1515.
[19] Baia L, Gigant K, Posset U, Schottner G, Kiefer W, Popp J. Applied Spectroscopy 2002;56:5.
[20] Spells SJ, Reinecke H, Sacristan J, Yarwood J, Mijangos C. Macromolecular Symposium 2003;203:147.
[21] Lin-Vien D, Colthup NB, Fateley WG, Grasselli JG. The handbook of infrared and Raman characteristic frequencies of organic molecules. San Diego: Academic Press; 1991.
[22] Nyquist RA. Interpreting infrared, Raman, and nuclear magnetic resonance spectra, vol. 1. San Diego: Academic Press; 2001.
[23] Nyquist RA. Interpreting infrared, Raman, and nuclear magnetic resonance spectra, vol. 2. San Diego: Academic Press; 2001.
[24] Sipani V, Scranton AB. Journal of Polymer Science Part A Polymer Chemistry 2003;41:2064.
[25] Hill LW. Journal of Coatings Technology 1992;64:29.
[26] Menard KP. Dynamic mechanical analysis: a practical introduction. Boca Raton: CRC Press; 1999.